# Quasi-Yagi Microstrip Dipole Antenna with Circular Arc Parasitic Elements for Wireless Sensing Networks

***Tiago E.S. Oliveira*[1]*, João R. Reis*[2]*, and Rafael F.S. Caldeirinha*[2]**

[1]Polythecnic of Leiria, Leiria, Portugal

[2]Instituto de Telecomunicaçoes, Leiria, Portugal
Email: rafael.caldeirinha@ipleiria.pt

## Abstract

In this paper, a Quasi-Yagi microstrip dipole antenna with circular arc parasitic elements for wireless sensing networks is presented. With the aim of being employed in a multi-sector base-station (BS) of a Wireless Sensing Network (WSN), the proposed antenna is designed and optimised to operate in the 2.4 GHz ISM band. Specific project requirements, such as: operating frequency, gain, half power beam-width (HPBW) and, consequently, Field of View (FOV) are taken into consideration when dimensioning the antenna. After proper design optimization, carried out with the aid of a full wave electromagnetic solver (CST Microwave Studio), an antenna prototype has been fabricated and experimentally characterized inside an anechoic chamber. From the measurement results obtained with the prototype, the antenna yields to a realised gain of 8.6 dBi, an HPBW of 64° and 42° in the azimuth and elevation planes, respectively, and a back-to-front ratio of 16.4 dB, at 2.44 GHz. The measurement results are proved to be in good agreement with the simulation ones.
*Index Terms:* Antenna, Quasi-Yagi, WSN, Base-Station, Director, Circular Arc.

## 1. Introduction

Wireless Sensor Networks (WSNs) are nowadays widely implemented [1], often being offered as a solution for monitoring networks, in particular for: environment monitoring [2], [3], security [4], [5], health monitoring [6], [7], agricultural [8], [9], hazard detection [10], among many others. A WSN is typically arranged in a point to multi-point configuration, composed of a collection of a large number of Sensor Nodes (SN) that are scattered in a certain monitoring area [11] and, a Base Station (BS) which collects the nearby environment data and forward it to higher layer network or upload to a Cloud service for further analysis.

In the majority of WSN applications, it is desirable to have a BS covering all its surroundings, typically requiring a Field of View (FOV) of 360 degrees. Antennas that exhibit an omnidirectional radiation pattern, e.g. dipole or monopole antennas, can fit the purpose, offering however, relatively low gains, which consequently impact the dynamic range of the system. To overcome this issue there are many techniques known in the literature, as e.g. beamforming, beamsteering and antenna sectorisation.

In particular, antenna sectorisation comprehends the division of the area (cell) covered by the antenna radiation pattern, in sub-sectors, so that higher directivity antennas with lower FOV can be employed [12]. Ultimately, the number of sectors depends on the half power beam-width (HPBW) of a single element antenna [13].

To this extend, it is proposed in this paper a novel microstrip quasi-Yagi antenna, based on the Yagi-Uda antenna principle. These antennas typically present relatively high gain, depending on the number of elements used, and moderate front-to-back ratio [14], ideal for the proposed application. In fact, Yagi-Uda antennas are very well known and their design procedure is well established from many years ago [15]. These end-fire antennas are typically composed of parallel metallic rods acting as reflector and directors of a driven element and, widely used for terrestrial television broadcasting services, in the HF, VHF and UHF bands [14]. Due to its popular design, they have rapidly been adapted to microstrip technology, by etching the directors and reflector directly in dielectric substrates [16], [17]. In recent years, several authors have been evolving this particular antenna design or constructed new antennas based on its physical principle. For example in [18], the authors have suggested a cloaked Yagi-Uda design, by introducing novel radiator designs, capable of being electromagnetically undetectable in another desired frequency range. In [19], the authors recurred to Square-Shaped Split Ring Resonators (SRRs) to reduce the width of planar Yagi-Uda antennas. In [20], the authors developed a wideband beam-switchable quasi-Yagi antenna array

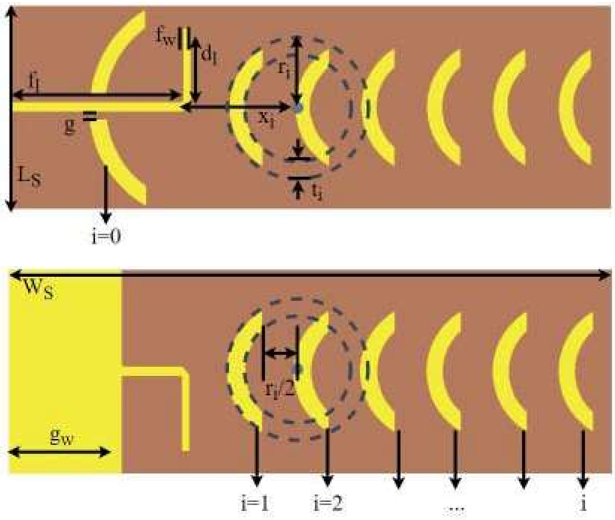


**Figure 1. Proposed circular arc Quasi-Yagi antenna layout: (a) top view and (b) bottom view.**

operating at 28 GHz, for mobile handsets. The proposed architecture consists of five quasi-Yagi antennas printed on Rogers substrate. More recently in [21], the authors have presented a three-port vertically polarized Quasi-Yagi Multiple-Input-Multiple-Output (MIMO) with pattern diversity for 5G N78 band applications. In this paper, it is proposed a novel quasi-Yagi antenna design based on circular arc shaped directors and reflector. Design guideline and simulation workout is presented for the antenna operating in the 2.4 GHz band, aiming at least 9 dBi of gain, a HPBW of 60 degrees, and a back-to-front ratio greater than 15 dB.

This paper is organised as follows: In Section II the antenna layout is thoroughly described. Section III presents in detail the parametric simulation and subsequent antenna optimisation, using a full wave electromagnetic solver (CST Microwave Studio). In section IV, the experimental setup considered for antenna characterisation is described, followed by subsequently analysis and discussion of the experimental results obtained from the prototype. Finally, in Section V the main conclusions are drawn.

## 2. Antenna Layout

The proposed antenna is depicted in Figure 1. It is based on a Yagi-Uda antenna design applied to microstrip technology, in which metallic parasitic elements are used as directors and reflector, in order to focus the radiated energy in one direction. The antenna is composed of a microstrip dipole, a circular arc shaped reflector over a ground plane (defined by $gw$) and, six circular arc shaped directors. The circular arc shaped reflector and directors should be seen as a quarter of a circle centred at $x_i$ with radius $r_i$ and thickness $t_i$, where $i$=0,1,2,... represents the number of the of the reflector/director, as depicted in Figure 1. The overall antenna dimensions are dictated by the parameters $W_S$ x $L_S$. The feeding line width ( $f_w$ ) and length ( $f_l$ ) dictates the input impedance of the antenna, while the frequency of operation is defined by the dimensions of the dipole arms ( $d_l$ ). The dipole arms are perpendicular to the feeding line thus, creating a 90° bend which can cause an unnecessary signal reflection to the source. To overcome this issue the bend was mitred, to reduce the capacitance of the line, maintaining the desired impedance. The antenna was designed in a double-sided FR4 substrate with $\varepsilon_r$ =4.4, a loss tangent of 0.014 and a thickness of $h$ =1.6 mm. The optimisation of the antenna dimensions and the number of directors are further analysed and discussed next section.

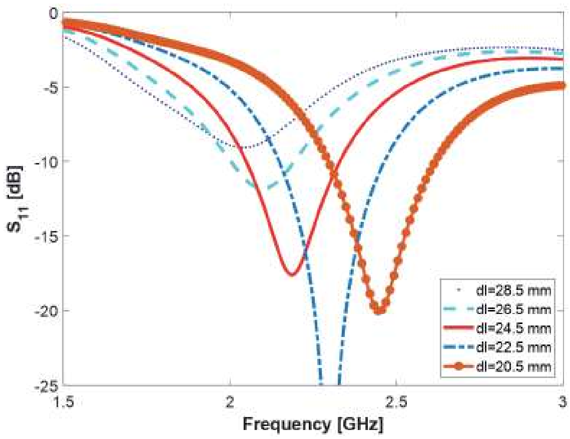


**Figure 2. Simulated S11-parameter for several values of dl, within the selected parametric range.**

## 3. Design and Optimisation

The proposed antenna design configuration was dimensioned with the assist of a full wave electromagnetic solver (CST MWS), in an iterative design approach. In a first iteration, the feeding element, *i.e.* the microstrip dipole was evaluated isolated (without directors and reflector), in order study the impact of the length of the dipole arm in $S_{11}$ performance and, find the optimum value for antenna resonating at 2.44 GHz (target frequency). Therefore, a parametric study was carried out on $d_l$, with the initial value being set at λg/8 and by fixing $gw$ at 32 mm, $L_S$ = 61 mm and $f_l$ = 52 mm. While $L_S$ was defined to accommodate at least the arms length (i.e. 2× $\lambda g/8$), $f_l$ and $gw$ were deliberately defined to further accommodate the reflector shape. $f_w$ was set at 3.1 mm corresponding to a 50Ω impedance line for the proposed substrate. The simulation results of the parametric study are depicted in Figure 2. The parametric simulation run within the range of 20.5 to 28.5 mm, with 2 mm step. From the results, it is possible to observe that $d_l$ = 20.5 mm is the optimised value for the desired resonance frequency (*i.e.* 2.44 GHz). With the dipole arms length already defined, the next step in the antenna design is to evaluate the impact of adding the directors in antenna performance. Therefore, a single director was added to the feeding antenna, at the position $x_1$ = 32 mm. At this point, no reflector has been considered. The initial values of $t_1$ =8 mm and $r_1$ = 22 mm were considered as starting point for the optimisation. The addition of the director provoked two effects in the antenna

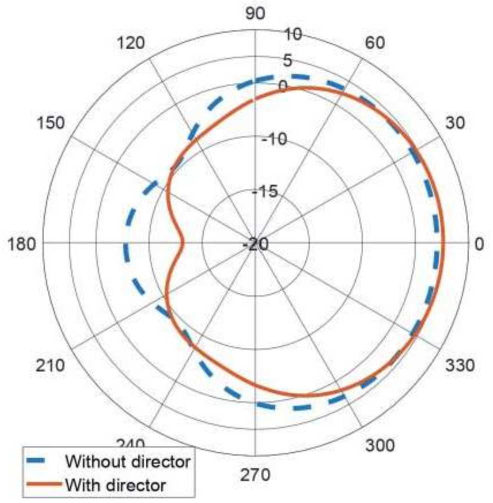


**Figure 3. Impact of the addition of a single director in the antenna radiation pattern (in azimuth plane), at 2.44 GHz.**

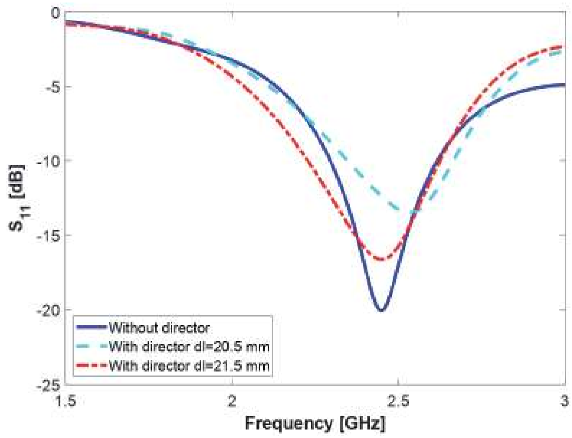


**Figure 4. Impact of the addition of a single circular arc shaped director in S11-parameter.**

performance: an increase in the overall gain (Figure 3) and an undesirable deviation of the antenna's resonating frequency, as well as an increase of the $S_{11}$ amplitude (Figure 4). While the first effect was expected (in line with the concept of Quasi-Yagi antenna), the latter is thought to be associated with mutual coupling between the driven element (dipole) and the added director. To correct this frequency shift, the length of the dipole arms $d_l$ was optimised to 21.5 mm.

After ensuring the antenna was resonating at the desired frequency, a parametric study was carried out in all parameters of the circular arc director ($r_1$, $x_1$ and $t_1$). The study aims to optimise the circular arc director dimensions to achieve the greatest antenna gain possible, while ensuring the antenna is still operating at the target frequency. From an extensive parametric study, it was found that the results which best favour the antenna performance in terms of gain are: $x_1$ = 36 mm, $t_1$ =5 mm and $r_1$ = 21 mm. From Figure 5, it is possible to observe that such values yield a realised gain of 6.02 dBi, which mean an increase of 1.65 dB, when compared to the antenna layout without a director. Furthermore, different director shapes, such as the typical rectangular and, inverted circular arc shape, were also studied and optimised with the aid of several parametric simulations (not included in this paper due to space constraints). The simulated radiation patterns in the azimuth plane for the mentioned shapes (also optimized), are presented in Figure 6. When comparing the results, is clear that the circular arc shapes slightly improve the overall gain of the antenna, the addiction of a director with the rectangular shape generated a gain of 5.6 dBi, whereas for the inverted circular arc shape a gain of 5.86 dBi is presented and, as previously mentioned, the circular arc shape yields a realised gain of 6.02 dBi. The latter, not only

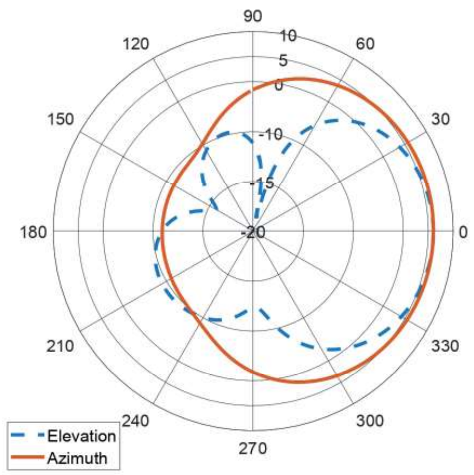


**Figure 5. Radiation pattern in azimuth and elevation planes, at 2.44 GHz, for the optimised antenna with a single director.**

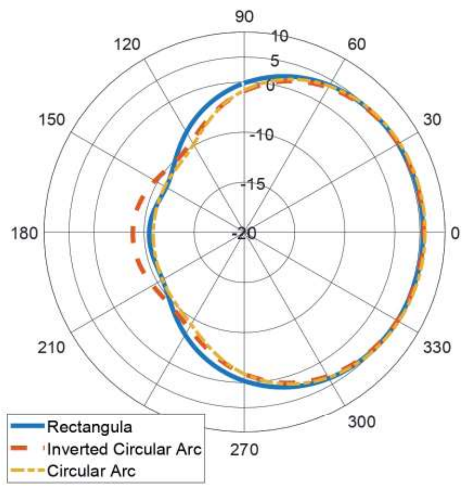


**Figure 6. Radiation pattern in azimuth plane, at 2.44 GHz, for different optimised director shapes.**

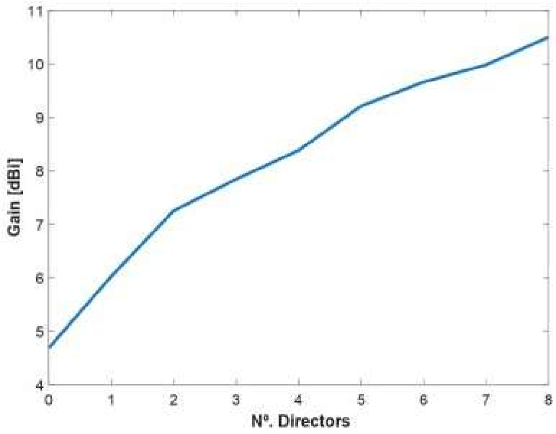


**Figure 7. Variation of the realised gain against the number of directors.**

presents the highest gain but also the best back-to-front ratio of 17 dB, therefore the circular arc shape was chosen.

Aiming to design an antenna with a higher gain, the process of adding directors has been studied. Thus, a parametric workout was carried out to access the gain improvement against the number of directors (with the same dimensions). The directors were added progressively to the layout, at the position $x_i = x_{i-1} + 18$ mm. The maximum gain at the antenna boresight has been obtained, and it is plotted against the number of directors (up to 8) in Figure 7. From the analysis of the results, it can be seen that after the addition of 6 directors, the ratio between gain and number of directors decreases. The difference from 6 to 8 directors is 0.81 dB, while the difference from 4 to 6 is 1.24 dB. Thus, for the best trade-off between antenna dimensions and gain, it was opted for 6 director design which achieves the target gain of 9.6 dBi. This represents an additional gain of 3.6 dB, when comparing with the configuration of a single director.

To further improve the front-to-back ratio of the antenna (already considering 6 directors), an additional circular arc shape was added to the design. The element was added prior to the feeding line (at the position $x_0$ =8 mm), over the ground plane, acting as a reflector. The dimensions of the reflector were also optimised using CST MWS with the goal of improving the front-to-back ratio. From the parametric workout, it was found that the best front-to-back ratio is of 18.63 dB, achieved with $r_0$ = 34.5 mm, $x_0$ = 8 mm, $t_0$ = 5 mm and $g$ = 2 mm, as depicted Figure 8, which improves 4.28 dB, from the case without reflector (Figure 8a). However, this change came at the expense of significantly increasing the side-lobe-levels, as it can be observed from the radiation patterns of Figure 8b. This indicates that most of the energy being reflected by the reflector is being re-radiated towards the side lobe direction, instead of the boresight direction, thus justifying the small increase of gain (only 0.1dB) of the main lobe. Please note that if the intention was exclusively increasing the gain of the main lobe, this could have been done by slightly shaping the reflector, e.g. making it more parabolic.

Finally, after all the design optimisation performed in this section, an antenna with an overall size of 175 × 61 mm$^2$, and dimensions (in mm): $L_S$ = 61, $W_S$ = 175, $f_l$ = 52, $x_0$ = 8, $g$ = 2, $r_0$ = 34.5, $t_0$ = 5, $f_w$ = 3.1, $t_i$ = 5, $r_i$ = 21, $x_1$ = 36, $x_2$ = 54, $x_3$ = 72, $x_4$ = 90, $x_5$ = 108, $x_6$ = 126, $gw$ = 32 and $d_l$ = 21.5, presents a realised gain of 9.7 dBi,a total efficiency of -0.55 dB (89%), a front-to-back ratio of 18.63 dB and, a HPBW (FOV) of 60$^\circ$. The polarization is vertical with the E-field parallel to the dipole arms

# 4. Experimental Characterisation

## 4.1. Setup

In order to experimentally characterise the proposed antenna, the prototype depicted in Figure 9 was fabricated. Firstly, antenna matching was evaluated by measuring the $S_{11}$-parameter, using a Vector Network Analyzer (VNA) (R&S ZVM). Subsequently, several antenna radiation

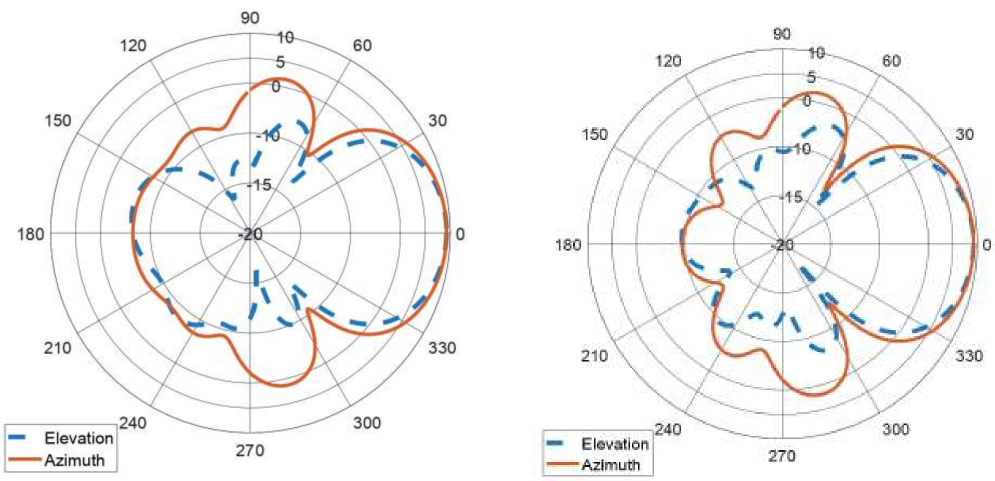


**Figure 8. Radiation pattern in azimuth and elevation planes, at 2.44 GHz, (a) without and (b) with the reflector.**

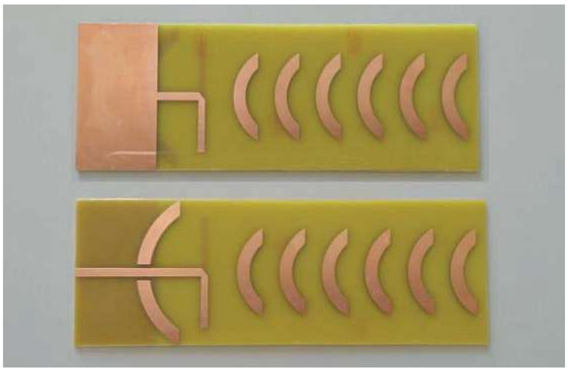

**Figure 9. Photography of the Quasi-Yagi microstrip dipole antenna with circular arc parasitic elements prototype.**

patterns, in the two main antenna planes, *i.e.* azimuth and elevation, have been obtained. To this end, the setup of Figure 10a was assembled inside an anechoic chamber enabling experiments to be performed in a controlled, electromagnetically quiet and reflection free radio environment.

In particular, a well characterised *Aaronia Hyperlog 30100* antenna was used as the Tx antenna (Figure 10b). It is connected to a Signal Generator (R&S SMR27) producing a continuous wave (CW)), with a transmission power of 0 dBm. At the receiver end, a well characterised *Aaronia Hyperlog 60100* antenna was connected to a spectrum analyser (Agilent E4407B) to be used as reference, later replaced by the antenna under test (AUT). The antennas were placed 3,5 meters apart, ensuring that the measurement took place in the far-field region of the antennas. The Tx antenna was kept fixed throughout the measurements, while the AUT was rotated around its axis with the assist of motorised pan/tilt head unit. The received power was acquired for each angular step with 1° of resolution, within the range defined between -180° and 180° (in the azimuth plane). Both Tx and Rx antennas were further rotated 90° to measure the radiation pattern in the elevation plane, using the same physical setup. The received power acquisition and movement control were executed in real-time and post processed in MATLAB, using a software developed for the effect.

## 4.2 Experimental Results

From the experimental $S_{11}$, depicted in Figure 11, it is possible to observe that the measured results are in good agreement with the simulated ones. Even though the $S_{11}$ presents slightly difference around the resonance peak at 2.4 GHz, antenna matching is still below -10 dB, presenting a bandwidth of 390 MHz, defined between 2.12 to 2.51 GHz, in experiments, against a slightly larger bandwidth of 420 MHz in simulations. Such discrepancy can be associated to mismatched values of the permittivity of the substrate between the real data and the one provided by the manufacturer, accuracy issues associated with the

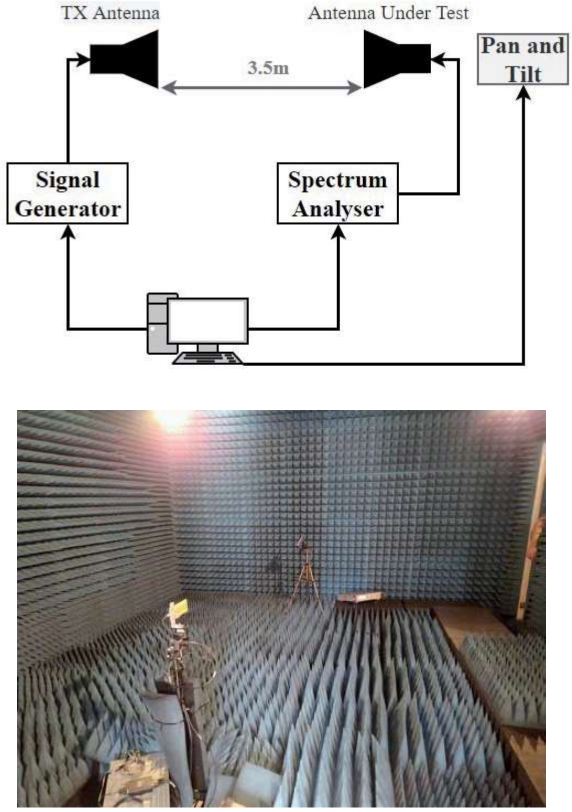


**Figure 10. Radiation pattern experimental characterisation setup (a) diagram and (b) photography**

PCB production technique (produced in-house), and the use of the SMA connector, not considered in simulations.

In terms of the radiation pattern obtained at 2.44 GHz, depicted in Figure 11b and Figure 11c for the azimuth and elevation planes, respectively, it can be observed a good agreement in the shape, between the simulation and measured results. According to experiments, the antenna presents a total gain of of 8.6 dBi, an HPBW of 64° in azimuth and 42° elevation planes, respectively, and a back-to-front ratio of 16.4 dB. This compares to simulations by having a decrease of 1.1 dB in total gain and 2.2 dB in back-to-front ratio. HPBW in simulations also decreases by 5° in both azimuth and elevation planes.

## 5. Conclusions

A novel Quasi-Yagi Microstrip Dipole antenna with circular arc parasitic elements is proposed in this paper. The antenna is comprised of a microstrip dipole used as the driven element, a circular arc shaped reflector and six equal circular arc shaped directors. A parametric study on several antenna parameters, including the shape and the number of directors, is performed in order to meet specific project requirements (operating frequency, gain, HPBW and back-to-front ratio). After proper antenna optimisation using CST MWS, an antenna prototype designed to operate at 2.44 GHz has been fabricated in FR4 substrate. The

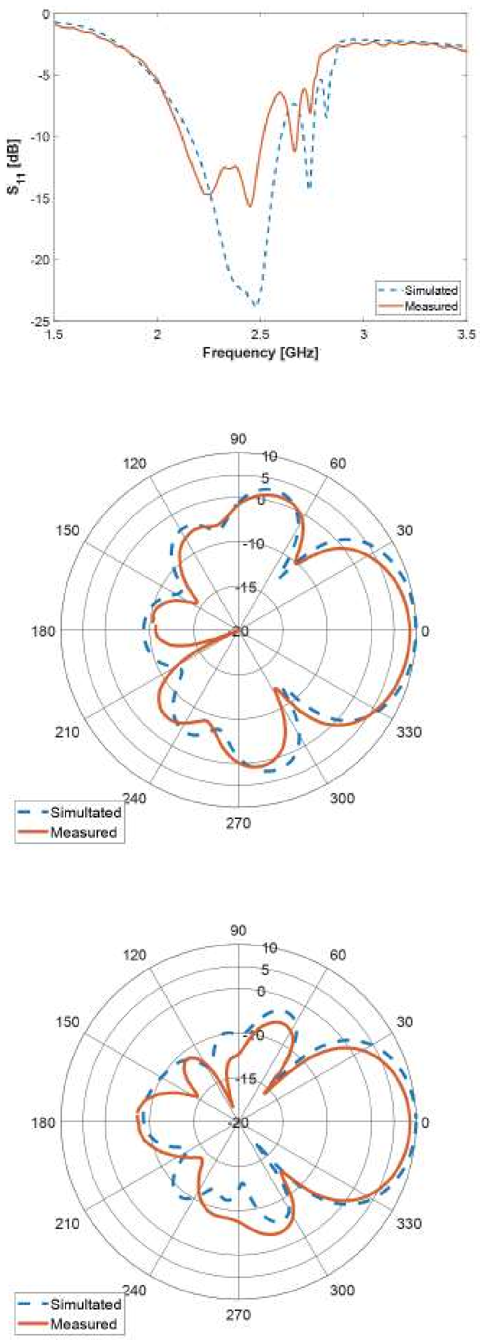


**Figure 11. Simulated and measured results for the (a) S11-parameter and, radiation patterns at (b) azimuth and (c) elevation planes.**

antenna presents overall dimensions of 175×61 $mm^2$. Further experimental characterisation carried out inside an anechoic chamber ensured a total gain of 8.6 dBi, a bandwidth of 390 MHz (from 2.12 to 2.51 GHz), HPBW of 64° in azimuth and 42° elevation planes, respectively, and a back-to-front ratio of 16.4 dB. Giving its technical characteristics and the end-fire radiation pattern, this antenna will enable the development of compact multi-sector base stations using circular array, as opposed to multiple flat panels, typically of large volumes, as the ones proposed in [22] and [23]. Further work will aim at antenna implementation in a multi-sector WSN base-station, composed of 6 Quasi-Yagi elements, which will be further tested in a real-world scenario, *i.e.* implemented in a wireless sensing network.

## Acknowledgement

This research was partially under the project WSN-EM: PTDC/EEI-EEE/30539/2017 by FCT/MCTES through national funds, and when applicable, by EU funds under the project UID/EEA/50008/2021.

## References


1. M. L. Laouira, A. Abdelli, J. B. Othman, and H. Kim, "An efficient WSN based solution for border surveillance," *IEEE Transactions on Sustainable Computing*, vol. 6, no. 1, pp. 54–65, jan 2021.

2. B. Montrucchio, E. Giusto, M. G. Vakili, S. Quer, R. Ferrero, and C. Fornaro, "A densely-deployed, high sampling rate, open-source air pollution monitoring WSN," *IEEE Transactions on Vehicular Technology*, vol. 69, no. 12, pp. 15 786–15 799, dec 2020.

3. O. B. Gonzalez and J. Chilo, "WSN IoT ambient environmental monitoring system," in *2020 IEEE 5th International Symposium on Smart and Wireless Systems within the Conferences on Intelligent Data Acquisition and Advanced Computing Systems (IDAACS-SWS)*. IEEE, sep 2020.

4. H. Luo, K. Wu, Z. Guo, L. Gu, and L. M. Ni, "Ship detection with wireless sensor networks," *IEEE Transactions on Parallel and Distributed Systems*, vol. 23, no. 7, pp. 1336–1343, jul 2012.

5. S. Astapov, A. Riid, and J.-S. Preden, "Military vehicle acoustic pattern identification by distributed ground sensors," in *2016 15th Biennial Baltic Electronics Conference (BEC)*. IEEE, oct 2016.

6. Y. Zhang, L. Sun, H. Song, and X. Cao, "Ubiquitous WSN for healthcare: Recent advances and future prospects," *IEEE Internet of Things Journal*, vol. 1, no. 4, pp. 311–318, aug 2014.

7. G. Hernandez-Penaloza, A. Belmonte-Hernandez, M. Quintana, and F. Alvarez, "A multi-sensor fusion scheme to increase life autonomy of elderly people with cognitive problems," *IEEE Access*, vol. 6, pp. 12 775–12 789, 2018.

8. D. D. K. Rathinam, D. Surendran, A. Shilpa, A. S. Grace, and J. Sherin, "Modern agriculture using wireless sensor

network (WSN)," in *2019 5th International Conference on Advanced Computing & Communication Systems (ICACCS)*. IEEE, mar 2019.

9. D. Qiong and P. Hao, "Design and implementation of irrigation water saving control system based on WSN," in *2021 International Conference on Intelligent Transportation, Big Data & Smart City (ICITBS)*. IEEE, mar 2021.

10. L. Shu, Y. Chen, Z. Sun, F. Tong, and M. Mukherjee, "Detecting the dangerous area of toxic gases with wireless sensor networks," *IEEE Transactions on Emerging Topics in Computing*, vol. 8, no. 1, pp. 137–147, jan 2020.

11. L. K. Ketshabetswe, A. M. Zungeru, M. Mangwala, J. M. Chuma, and B. Sigweni, "Communication protocols for Wireless Sensor Networks: a survey and comparison," *Heliyon*, vol. 5, no. 5, p. e01591, may 2019.

12. M. Appleby and F. Harrison, "47 -Cellular radio systems," in *Telecommunications Engineer's Reference Book*, F. Mazda, Ed. Butterworth-Heinemann, 1993, pp. 47–1–47–17.

13. T. E. S. Oliveira, J. R. Reis, M. Vala, and R. F. S. Caldeirinha, "High performance antennas for early fire detection wireless sensor networks at 2.4 GHz," in *2021 IEEE-APS Topical Conference on Antennas and Propagation in Wireless Communications (APWC)*. IEEE, aug 2021.

14. C. A. Balanis, *Antenna Theory: Analysis and Design, 3rd Edition*. John Wiley & Sons, 2005, vol. 72.

15. H. YAGI and S. UDA, "Projector of the sharpest beam of electric waves," *Proceedings of the Imperial Academy*, vol. 2, no. 2, pp. 49–52, 1926.

16. Y. Ding, Y. C. Jiao, P. Fei, B. Li, and Q. T. Zhang, "Design of a multiband quasi-Yagi-type antenna with CPW-to-CPS transition," *IEEE Antennas and Wireless Propagation Letters*, vol. 10, pp. 1120–1123, 2011.

17. K. D. Xu, D. Li, Y. Liu, and Q. H. Liu, "Printed quasi-Yagi antennas using double dipoles and stub-loaded technique for multi-band and broadband applications," *IEEE Access*, vol. 6, pp. 31 695–31 702, 2018.

18. A. Monti, J. Soric, A. Al`u, A. Toscano, and F. Bilotti, "Design of cloaked Yagi-Uda antennas," *EPJ Applied Metamaterials*, vol. 3, p. 10, 2016.

19. P. Aguila, G. Zamora, S. Zuffanelli, F. Paredes, F. Martin, and J. Bonache, "Reducing the width of planar Yagi-Uda antennas using square-shaped split ring resonators (SRRs)," in *2017 11th European Conference on Antennas and Propagation (EUCAP)*. IEEE, mar 2017.

20. C. Di Paola, S. Zhang, K. Zhao, Z. Ying, T. Bolin, and G. F. Pedersen, "Wideband beam-switchable 28 GHz quasi-Yagi array for mobile devices," *IEEE Transactions on Antennas and Propagation*, vol. 67, no. 11, pp. 6870–6882, 2019.

21. Y. Xu, Y. Dong, S. Wen, and H. Wang, "Vertically polarized quasi-Yagi MIMO antenna for 5G n78 band application," *IEEE Access*, vol. 9, pp. 7836–7844, 2021.

22. P. Liu, J. Zhang, S. Lu, and J. Lin, "Design and achievement of miniaturization in Wi-Fi base station antenna," in *Proceedings of 2014 3rd Asia-Pacific Conference on Antennas and Propagation*. IEEE, jul 2014.

23. J.-N. Lee, K.-C. Lee, and P.-J. Song, "The design of a dual-polarized small base station antenna with high isolation having a metallic cube," *IEEE Transactions on Antennas and Propagation*, vol. 63, no. 2, pp. 791–795, feb 2015.